

K_{α} Emission Induced by X-rays from Laser-Produced Plasma

Naohiro YAMAGUCHI

Institute of Plasma Physics, Nagoya University, Nagoya 464

(Received)

Experiments are conducted to study the effects of x-ray radiation and suprathermal electrons produced by laser-produced plasma on the energy transport. Plasmas were produced by irradiating aluminum coated silicon targets (layered targets) with 1.06 μm Nd:glass laser of 10^{14} W/cm^2 power density. The nanosecond time resolved x-ray spectra (1.5 ~ 2.2 keV) were measured with the scintillator-photomultiplier array. The layer from which He-like ions are originated is limited to have a depth of 0.1 μm into the target, and the Si K_{α} line emitting region has a depth of about 1 μm . The duration of K_{α} line signal is longer than that of Al XII line ($1s2p^1P - 1s^2^1S$) signal. The K_{α} emission can be explained by x-ray absorption in the target material.

§1. Introduction

Energy transport phenomena in laser-produced plasmas are one of the important problems in the pellet fusion research. Smooth heating of the target in the lateral direction by thermal conduction is required to obtain a stable and uniform compression. Preheating of the interior of laser-irradiated targets by either suprathreshold electrons or x-rays would make difficult to compress a fuel core. Electrons or x-rays of sufficient energy travelling into cold un-ionized material can eject K-electrons.¹⁾ A K-shell vacancy decays by emitting either a K_{α} photon with a probability called fluorescence yield or an Auger electron which cannot escape from the target. The fraction into the Auger cascades is mostly converted into heat. Therefore, the K_{α} radiation could be used as a measure of absorbed energy in the interior of the target. A few experiments have been done from this aspect.^{2),3)} Especially in a layered target experiment³⁾ the role of x-ray radiations has been ignored. The K_{α} line emission from laser-produced plasmas has usually been thought to be closely connected with suprathreshold electrons. However, a large amount of x-ray flux from a laser-produced plasma is expected,⁴⁾ so that the absorption in a solid density region should be taken into account.⁵⁾ It is necessary for the interpretation of energy transport process in a laser plasma to clarify the origin^{of} K_{α} x-ray generation. When materials with various atomic number (Z) are used as targets from the requirement of pellet design, highly stripped ions are generated and emit the characteristic x-ray line radiation. This attracts a

wide interest in atomic physics⁶⁾ and astrophysics.⁷⁾

The purpose of this experiment is to determine the origin of K_{α} radiations and to survey the structure of a plasma in over dense region of a target where the laser light cannot reach. To find the plasma spatial distribution in the direction normal to the target surface by means of x-ray spectroscopy, we use silicon plates coated with aluminum of various thickness as targets. Spectra from each layer provide a spatial resolution, which give data on the depth of K_{α} -emitting region. The multi-channel photoelectric detection of x-ray lines is performed for time resolved measurement, which enables us to separate the contributions of plasma x-rays to the K_{α} emission from that of fast electrons. This provides also wide dynamic range and sufficient sensitivity compared with x-ray film recording.

§2. Experimental Arrangement

The laser system used in this experiment is composed of a YAG mode-locked oscillator and six stage Nd:glass amplifiers. It delivers a pulse of 3 ± 1 J in 150 ps at 1.06 μm . The main pulse has a small prepulse less than 30 mJ in energy, 2 or 3 ns ahead. The output beam was focused via a 10 cm focal length, f/1.33 aspheric lens onto a plane target. Targets used were finely polished single-crystal silicon plates whose surface roughness was less than 0.01 μm (100 \AA), which was measured by a micro-interferometer, and also those coated with aluminum. The aluminum layer thickness was varied over the range 0.002 to 10 μm . Aluminum thickness less than 0.1 μm was monitored by a

vacuum deposition controller. Thickness of aluminum layer thicker than $0.1\mu\text{m}$ was measured by the micro-interferometer after deposition. In the present experiment, the laser power density at the target surface was kept at around $3 \times 10^{14} \text{ W/cm}^2$ with a focal spot diameter of $80 \mu\text{m}$.

The x-rays from the laser-produced plasma through a $25 \mu\text{m}$ thick Be window were analyzed by a Hámos type⁸⁾ PET crystal ($2d = 8.742 \text{ \AA}$, d is the atomic layer spacing) which was a cylindrically curved crystal ($R = 101.6 \text{ mm}$, R is the radius of curvature). The schematic arrangement of this experiment is illustrated in Fig.1. The plasma which was regarded as a point x-ray source was produced at the center of crystal curvature so that the x-ray was incident at a Bragg angle in the range 38° to 66.5° on the crystal. The exit apertures for measurement were set along the cylindrical axis of the curved PET crystal. In this way the reflected x-ray converges orthogonal to the dispersion and the enhancement in x-ray spectrum intensity is performed. The wavelength range 5.5 to 8 \AA was covered by this spectrometer. The spectral resolution is 0.005 \AA limited by an x-ray source dimension and by the roughness of crystal surface. The dispersion is 0.015 \AA/mm . X-ray films were used to identify the x-ray spectra (Fig.2). The time-resolved intensity measurement of the x-ray lines was made with the scintillator-photomultiplier array (Fig.1). Each plastic scintillator (NE 110) was formed in a small chip and was coupled with a photomultiplier (HTV R-654) through an optical fibre. The channel width is about 0.02 \AA determined by the exit slit width. This width sufficiently

covers individual x-ray lines, so that each channel corresponds to each x-ray line. The temporal resolution of this system is about 3 ns. This detection system has a dynamic range of 10^3 and is more sensitive than x-ray films or p-i-n diodes.

The four silicon p-i-n diodes behind Be foils of different thicknesses were set to view a plasma so that the target normal line-of-sight angle was about 8° . They always monitor the integrated x-ray intensity and the electron temperature. The foil thicknesses used were 200 μm , 400 μm , 800 μm and 3200 μm . The cut off energy of each foil defined as photon energy which gives zero transmittance in an extrapolated filter transmission curve versus photon energy is 1.8 keV, 2.4 keV, 3.5 keV or 4.9 keV, respectively.

§3. Experimental Results

The laser energy is deposited into a plasma at the critical density region (where $n_e \sim 10^{21} \text{ cm}^{-3}$). Plasma heating occurs through the interaction of laser and plasmas,⁹⁾ and suprathermal electrons simultaneously produced.¹⁰⁾ The electron temperature, which was monitored during each shot, is determined by the absorption technique using four channel p-i-n diodes. The measured intensity ratios were fitted to the x-ray intensity ratio for the two temperature plasma. It has been found that the lower temperature component is $300 \pm 30 \text{ eV}$, the higher one is $4 \sim 6 \text{ keV}$ and the fraction of the higher temperature component is $(8 \pm 3) \times 10^{-7}$.

It can be thought from the recent spectroscopic

measurements¹¹⁾ that highly stripped ions are produced during the period of the laser energy deposition, then expand to the lower density region and decay into the lower stage of ionization through the recombination. The plasma dimension was measured from an x-ray microscope image transmitted through a 25 μm thick Be foil, using a toroidal mirror x-ray microscope.¹²⁾ The imaged x-ray is in the wavelength range 7 to 10 \AA where the helium-like resonance line is dominant. The region where helium-like ions emit x-rays is a disk like shape in front of the target surface, which is 50 μm thick and 250 μm in diameter. Typical densitometer trace of spectrograph for the aluminum coated silicon target is shown in Fig.2. One can see resonance lines, intercombination lines and satellite lines of Al and Si ions, and also Si K_{α} line. The observed Si K_{α} line (7.12 ± 0.012 \AA) is identified as the K_{α} line from the K-shell ionized silicon whose stage of ionization is from II to VI, at most.¹³⁾ Each line starts to rise almost simultaneously for every thickness of aluminum used. It takes about 3 nsec to reach the maxima of Al XII resonance line signals and the maximum of Si K_{α} line signal appears about 2 nsec later. Typical pulse waveforms of Al XII ($1s2p^1P - 1s^2 1S$) transition line and Si K_{α} line for 0.1 μm aluminum coated target are shown in Fig.3a. The Al XII resonance line might rise faster than 3 ns, but its signal waveform is restricted by the time response of the detection system. The important point to be stressed is not the absolute value of the signal rise time, but the difference in the peak time position between the Al XII line and Si K_{α} line which is

always found to exist even when each photomultiplier is exchanged. This temporal relation does not vary with the aluminum thickness used in this particular experiment. This is indicated in Fig.3b.

The Si K_{α} and Al XII first resonance (2^1P) line intensities normalized to the input laser energy are plotted in Fig.4 as a function of the aluminum layer thickness. Al XII (2^1P) line intensity increases as the aluminum thickness is increased from 0.002 μm to 0.1 μm and tends to saturate at 0.1 μm and above. The Si K_{α} line intensity remains constant for the aluminum layer thickness of less than 0.05 μm at the intensity level for the pure silicon target case, which is denoted by an arrow in Fig.4. Beyond 0.05 μm thickness of aluminum, Si K_{α} line intensity decreases monotonically. It is to be noted that the Si K_{α} signal may be smeared with the continuum x-ray mixing into the Si K_{α} channel. The continuum intensity involved in the K_{α} channel was estimated at one tenth or less of the maximum K_{α} intensity from the signals of Si K_{α} channel and neighbouring line-free channel for a silicon target. It is presumed that the continuum intensity remains almost constant for the layered target used. Besides, when the aluminum layer thickness increases, the Si K_{α} x-ray which comes out from a silicon substrate through the aluminum layer suffers from an attenuation by aluminum. Therefore, the correction has to be made about the continuum background and the attenuation by aluminum. The dashed curve in Fig.4 indicates thus corrected Si K_{α} line intensity as a function of the aluminum thickness. For aluminum thickness more than 3 μm the Si K_{α} line attenuation by aluminum is very

large, so that one can regard the Si K_{α} channel signal nearly the continuum signal. It is difficult to reduce the corrected K_{α} line intensity from the data obtained for more than 3 μm aluminum layered targets.

The normalized pulse waveforms of Si XIII (2^1P), Al XII (3^1P) lines and continuum x-ray about 2 keV are shown in Fig.5. They are the most effective x-rays in the vicinity of spectrum range of for K-shell ionization of silicon which is in the energy range from 1.8 to 2.4 keV. Typical intensities of these lines and continuum are summarized in Table I, which were measured for a silicon target.

§4. Discussion

4-1. Interpretation of the results

It has been considered that the so-called "suprathermal electrons" are produced through the laser light absorption in a plasma.¹⁰⁾ The equipartition time¹⁴⁾ between suprathermal component ($T_{eh} \sim 6 \text{ keV}$) and thermal one ($T_{e1} \sim 300 \text{ eV}$) is estimated to be as short as 10ps at the crytical density ($n_e \sim 10^{21} \text{ cm}^{-3}$). Therefore, the life time of suprathermal electrons is of the order of the input laser pulse duration, 0.15 ns in this experiment. Besides, the life time of a silicon K-shell vacancy is sufficiently short, which is about 10^{-14} s .¹⁵⁾ If the K_{α} transition is excited mairly by the suprathermal electrons, the duration of Si K_{α} line radiation is considered to be as 0.15 ns. The signal of Si K_{α} line must appear so that its peak rise time is limited by the time response of the detecting

device, that is about 3 ns. However, the measured Si K_{α} signal peak appears more than 3 ns later, which is clearly shown in Fig.3. Therefore, the assumption that the K_{α} x-ray is induced mainly by the suprathreshold electron is not valid. On the other hand, the composed pulse waveform of the x-ray lines and continuum which are able to ionize the silicon K electron resembles that of Si K_{α} line, as is seen in Fig.5.

It is found from the Si K_{α} intensity curve that a layer where the K-shell ionization takes place has about 1 μm depth. The depth of K_{α} emitting region is defined as the aluminum thickness for which the Si K_{α} line intensity decreases to one tenth of its maximum intensity. The constant Si K_{α} intensity for the thinner aluminum layer ($< 0.05 \mu\text{m}$) leads to an interpretation that a very thin layer just behind the target surface does not radiate the K_{α} x-ray. This can be seen in another experiment, too.³⁾ The decrease of Si K_{α} line intensity with the aluminum thickness can be explained by the attenuation of electrons or x-rays by the aluminum layer prior to their arrival at a silicon substrate. Hence, the depth of the Si K_{α} emitting region, which is found to be about 1 μm in this experiment (see Fig.4), should be related to the electron range or the x-ray absorption length in aluminum. The ranges for 300 eV electrons and 6 keV electrons are 0.006 μm and 0.4 μm , respectively.¹⁶⁾ These are too short to explain the K_{α} line intensity data. The thickness of aluminum by which a 2 keV x-ray intensity attenuated to one tenth of its initial intensity is about 2 μm . The transmission curve of a 2 keV x-ray in aluminum is qualitatively

similar to the experimental result shown in Fig.4. The results mentioned above indicate that the x-ray absorption by the target material is the most plausible candidate as the origin of K_{α} x-ray.

The dependence of helium-like resonance line intensity on the aluminum thickness shown in Fig.4 indicates that highly ionized ions originate from a region within $0.1 \mu\text{m}$ inside the target. This depth is thought to be connected with the penetration depth of laser-produced hot plasma.¹⁷⁾ The phenomena relevant to this depth are the thermal conduction in high density plasma and the production of highly stripped ions. Especially the ionization mechanism in a short period like a laser pulse width has not been clarified. The depth where highly stripped ions are generated is nearly the same as the range of suprathreshold electrons in aluminum, so that this depth seems to have some relation with suprathreshold electrons.

4-2. Mechanism of Si K_{α} line generation

The K-shell ionization mechanism in a solid target may be considered as the following: electrons and x-rays emitted from the hot plasma which always contacts with a solid surface of the target penetrate into cold un-ionized material and cause to ionize the K-electron of silicon atom. For simplicity, the case of the silicon target will be treated.

At first, the K-shell ionization efficiency, i.e. the number of K-shell ionization per one electron or photon, is to be estimated when an electron or an x-ray photon enters into the

target material. The analysis is nearly the same as that in an x-ray tube.¹⁸⁾ The K-shell ionization efficiency for an x-ray photon, n_{kx} , is written as

$$n_{kx} = (r_k - 1)/r_k, \quad (1)$$

where r_k is the K absorption-edge jump ratio. The K-edge jump ratio for silicon is 11.9,¹⁹⁾ so it follows that $n_{kx} = 0.92$.

The K-shell ionization efficiency for an electron whose initial energy is E_0 ($E_0 > E_k$) is written as

$$n_{ke}(E_0) = \int_{E_k}^{E_0} \frac{n_0 \sigma_k(E)}{(-dE/dx)} dE, \quad (2)$$

where n_0 is the target atom number density, $\sigma_k(E)$ is the K-shell ionization cross section by an electron impact, $(-dE/dx)$ is the electron energy loss and E_k is the K-edge energy. Using the Drawin's semi-empirical formula for $\sigma_k(E)$ ²⁰⁾ and the Thomson-Whiddington electron energy loss relation,²¹⁾ we obtain

$$n_{ke}(U_0) = 1 \times 10^{-24} \cdot \frac{n_0}{\rho} \left[\left(U_0 - \frac{\ln U_0}{2} - 0.22 \right) \ln U_0 - 0.78(U_0 - 1) \right], \quad (3)$$

where ρ is the density of the target material and $U_0 = E_0/E_k$.

In the case that electrons have the Maxwellian distribution, one can get an averaged K-shell ionization efficiency, $\langle n_{ke} \rangle_{kT_e}$, averaging over the Maxwellian distribution. After a simple numerical integration, the averaged efficiencies for the main plasma electrons and for the suprathermal ones are evaluated as

$\langle n_{ke} \rangle kT_e \sim 3 \times 10^{-7}$ ($kT_e = 300$ eV) and $\langle n_{ke} \rangle kT_e \sim 2 \times 10^{-1}$ ($kT_e = 6$ keV), respectively. The efficiency for x-rays is much higher than those for electrons.

In order to know the total K_α photon number, each efficiency has to be multiplied by the total incident x-ray photon number or electron number and the K-shell fluorescence yield. The number of x-ray photons in the energy range 1.8 to 2.4 keV which are effective for the silicon K-shell ionization is estimated to be of the order of 10^{12} from the integrated x-ray intensity measured with the filtered p-i-n diodes. One obtains the total plasma electron number to be 10^{17} at most, assuming that the volume in the target material (whose diameter and length are 200 μm and 1 μm , respectively) is fully ionized to the ionic charge of 14. The plasma column diameter is taken from the x-ray microscope photograph, and the length is to be equal to the depth of K_α line emitting region. This estimation gives an upper limit of the electron number. The suprathermal electron fraction is deduced from the p-i-n diode signals to be 10^{-6} of the bulk electrons, i.e. the thermal ones. Thus, we can get the ratio among the K_α line intensities induced by x-rays, by thermal electrons and by suprathermal electrons to be 100 : 3 : 2. It is clear that the K_α photon induced by x-rays is dominant.

In analyzing the K_α intensity for the layered target, one must take into account the transmission of the source electrons or x-ray photons. It is to be noted that the property of electron transmission in a material is different from that of x-ray transmission. Electrons transmitted through a layer of material

alter in the energy distribution from its initial one, while transmitted x-ray photons are not changed in energy. The expression of K_{α} photon number induced by electrons becomes more complicated.

The most effective x-ray are composed of the continuum in the energy range around 2 keV and the line radiations, that are Si XIII (2^1P), (2^3P) lines, Si XII satellites and Al XII (3^1P) line. The intensities of these lines and continuum are tabulated in Table I. Especially, the helium-like resonance line and the continuum take more than three-quarters of the total x-ray which is able to produce the K-shell vacancies in silicon. Although the Si He-like line intensities decrease for the thicker aluminum coated target, the Al XII resonance lines grow and compensate the decrease of the Si lines. As a result, it can be thought that the overall intensity of source x-ray for Si K_{α} x-ray production remains nearly constant for every layered target used in this experiment. The total K_{α} photon number induced by x-rays is

$$n_{K_{\alpha}} = \omega_k \frac{r_k - 1}{r_k} N_{ph} , \quad (4)$$

where ω_k is the fluorescence yield and N_{ph} is the number of absorbed x-ray photons whose energy is higher than E_k . Then, the ratio of the measured K_{α} line intensity to the relevant x-ray intensity should be limited to $\omega_k(r_k - 1)/2r_k$. It is calculated to be a value from 0.019 to 0.027, using the most reliable experimental and theoretical values of ω_k .²²⁾ The ratio obtained

the silicon target is about 0.02. It agrees well with the theoretical limit of K_{α} emission.

§5. Conclusion

X-ray spectroscopy with multichannel scintillator-photo-multiplier array was performed in a layered target experiment. The K_{α} x-ray emitting region is determined to be in the range from 0.05 μm to 1 μm inside the target surface by x-ray spectrum intensity measurement. It is found from the time resolved measurement of x-ray spectra that the K_{α} x-ray from target material has a little longer duration than the helium-like resonance lines. From qualitative consideration to the above experimental results and simple quantitative estimates, it is concluded that the K_{α} x-ray observed in this particular laser plasma experiment is induced mainly by the absorption of x-rays in a target material. Because the K_{α} photon number is proportional to the absorbed x-ray photon number (Eq.(4)), one can know directly the amount of transported x-ray energy by measuring the K_{α} photon number.

Acknowledgements

The author would like to thank Dr. M. Shiho and J. Mizui for collaboration and continuing discussions, and Dr. S. Aoki for providing the x-ray microscope photograph. Thanks are due to Professor J. Fujita, Dr. S. Uhtani and Dr. K. Kadota for stimulating and helpful discussions. Several valuable discussions

with Dr. T. Fujimoto and Dr. T. Kato are gratefully acknowledged. The author also would like to express his appreciation to Professor A. Miyahara and Professor K. Takayama for continuing encouragements and to Professor T. Yamanaka for the guidance on the design of the spectrometer. Thanks are also due to Mr. H. Yonezu for his technical assistance.

References

- 1) "Atomic Inner-Shell Processes": Vol.I, edited by B. Crasemann (Academic, New York, 1975)
- 2) B. Yaakobi, I. Pelah and J. Hoose: Phys. Rev. Lett. 37 (1976) 836
- 3) K. B. Mitchell and R. P. Godwin: J. Appl. Phys. 49 (1978) 3851
- 4) D. J. Nagel et al.: Phys. Rev. Lett. 33 (1974) 743
- 5) J. Mizui, N. Yamaguchi, T. Yamanaka and C. Yamanaka: Phys. Rev. Lett. 39 (1977) 619
- 6) V. A. Boiko, A. Ya. Faenov and S. A. Pikuz: J. Quant. Spectrosc. Radiat. Transfer 19 (1978) 11
- 7) B. C. Fawcett and R. W. Hayes: Mon. Not. R. astr. Soc. 170 (1975) 185
- 8) M. A. Blokhin: "Methods of X-ray Spectroscopic Research" (Pergamon, London, 1965)
- 9) W. L. Kruer in "Progress in Lasers and Laser Fusion" (Plenum, New York, 1975)
- 10) J. P. Freidberg, R. W. Mitchel, R. L. Morse and L. I. Rudsinski: Phys. Rev. Lett. 28 (1972) 795; P. Kolodner and E. Yablonovitch: Phys. Rev. Lett. 37 (1976) 1754
- 11) Yu. S. Kas'yanov, M. A. Mazing, V. K. Chevokin and A. P. Shevel'ko: JETP Lett. 25 (1977) 348; D. Landheer et al.: SPIE High Speed Photography 97 (1976) 207; F. E. Irons and N. J. Peacock: J. Phys. B. 7 (1974) 2084
- 12) Y. Sakayanagi and S. Aoki: Appl. Opt. 7 (1978) 601

- 13) L. L. House: *Astrophys. J., Suppl.* 18 (1969) 21
- 14) L. Spitzer, Jr.: "Physics of Fully Ionized Gases"
(Interscience, New York, 1965)
- 15) E. J. McGuire: *Phys. Rev.* 185 (1969) 1
- 16) O. Klemperer, A. Thetford and F. Lenz: *Proc. Phys. Soc.*
76 (1960) 705
- 17) B. Yaakobi and T. C. Bristow: *Phys. Rev. Lett.* 38 (1977)
350; M. H. Key et al.: Paper WA7, the Topical Meeting on
Inertial Confinement Fusion, San Diego, California, 1978
- 18) M. Green and V. E. Cosslett: *Proc. Phys. Soc.* 78 (1961)
1206, and *J. Phys. D* 1 (1968) 425
- 19) E. P. Bertin: "Principles and Practice of X-ray Spectro-
metric Analysis" (Plenum, New York, 1975)
- 20) C. J. Powell: *Rev. Mod. Phys.* 48 (1976) 33; H. W. Drawin:
Z. Phys. 164 (1961) 513 and *ibid.* 172 (1963) 429
- 21) R. Whiddington: *Proc. Roy. Soc. A* 86 (1912) 360
- 22) W. Bambynek et al.: *Rev. Mod. Phys.* 44 (1972) 716

Figure Captions

- Fig.1 Schematics of arrangement of a Hámos-type x-ray spectrometer and multichannel detector array.
- Fig.2 Densitometer trace of Al and Si spectra for 0.1 μm aluminum coated silicon target irradiated by a 2.9 J laser in 150 ps.
- Fig.3 (a) Typical signal pulse shapes of Al XII (2^1P) line and Si K_α line for 0.12 μm aluminum coated target. Each maximum is normalized to unity.
(b) The start-to-peak time of Al XII (2^1P) and Si K_α line signals as a function of thickness of aluminum layer. o: Si K_α ●: Al XII 2^1P
- Fig.4 Line intensities of Al XII (2^1P) and Si K_α as a function of the thickness of aluminum layer. An arrow at the left of the ordinate shows the Si K_α line intensity for a plane silicon target. A dashed curve is the Si K_α line intensity corrected for the continuum background and attenuation by an aluminum layer.
- Fig.5 Typical normalized pulse forms of the dominant x-rays above silicon K-edge energy, i.e. Si XIII (2^1P), Al XII (3^1P) and continuum in the energy range about 2 keV.

Table I. Signal Intensities of Si K_{α} line and x-rays, relevant to Si K_{α} production, measured by multichannel scintillator-photomultiplier systems.

Ion	SiXIII	SiXII	SiIII - SiVI
Transition	$1s2p^1P - 1s^21S$	$1s2p^3P - 1s^21S$	Satellites K_{α} Continuum
Energy (keV)	1.88	1.87	1.85 ~ 1.86 1.75 1.7 1.8 ~ 2.2
Detected signal	4800	~ 960 [†]	~ 480 [†] 180
voltage (mV)			20 ~ 2250 (per ^{††} channel)

[†] Estimated from the AlXII and AlXI spectra.

^{††} Channel width corresponds to about 3 eV.

$$I_{Si K_{\alpha}} / \int_{E_k}^{\infty} I_x d(h\nu) \approx I_{Si K_{\alpha}} / (I_{SiXIII} 2^1P + I_{SiXIII} 2^3P + I_{SiXII} sat. + \int I_{continuum} d(h\nu)) \sim 0.02$$

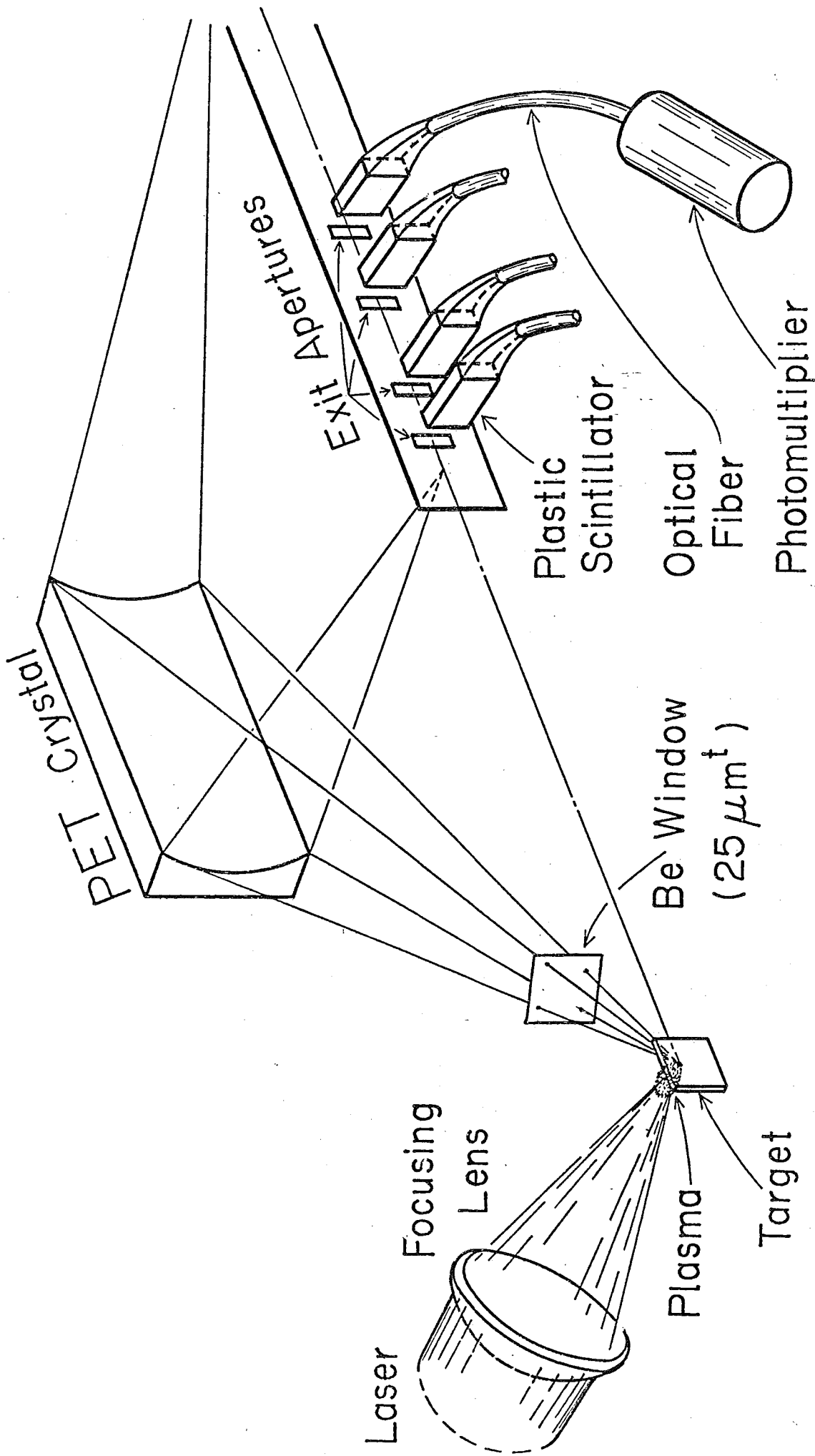


Fig. 1. Naohiro YAMAGUCHI (9)

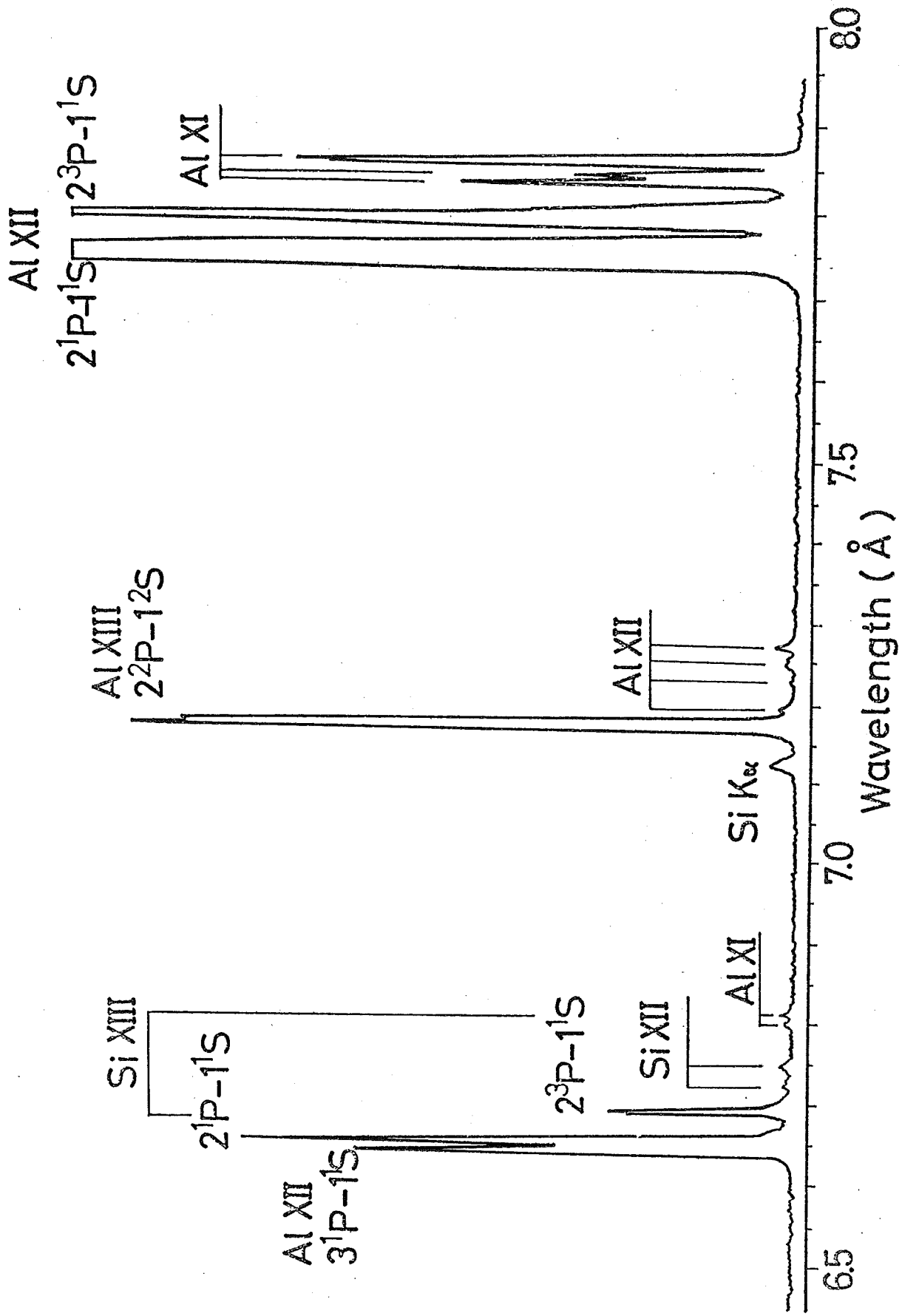


Fig. 2. Naohiro YAMAGUCHI (9)

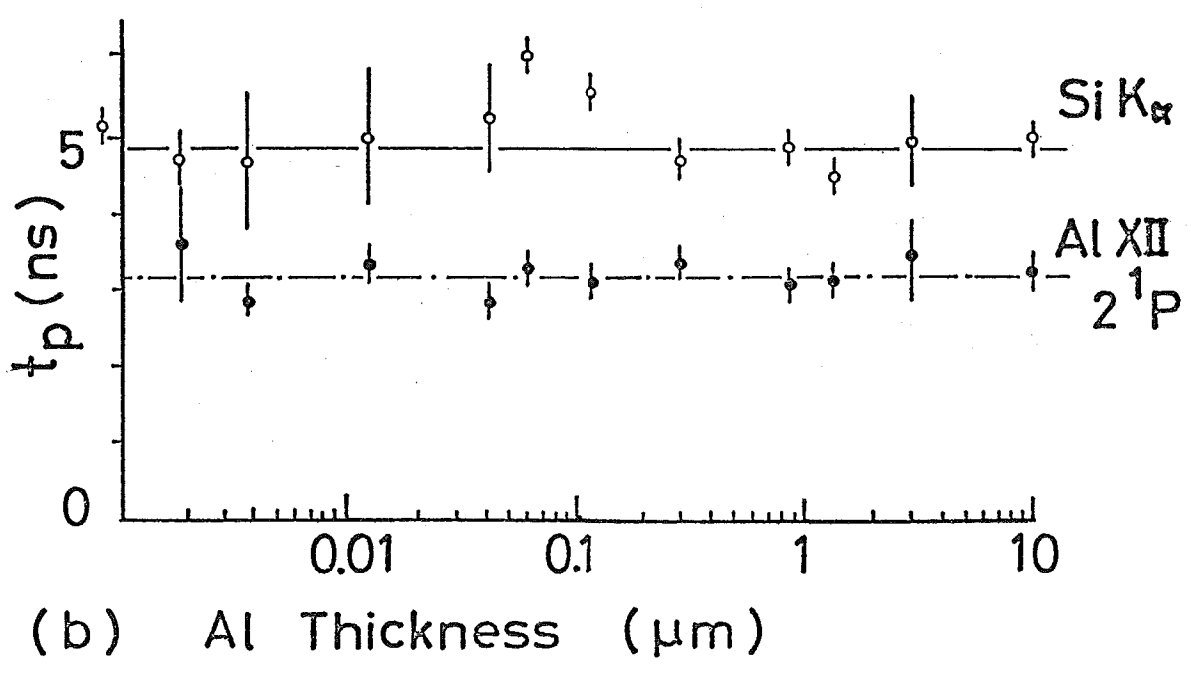
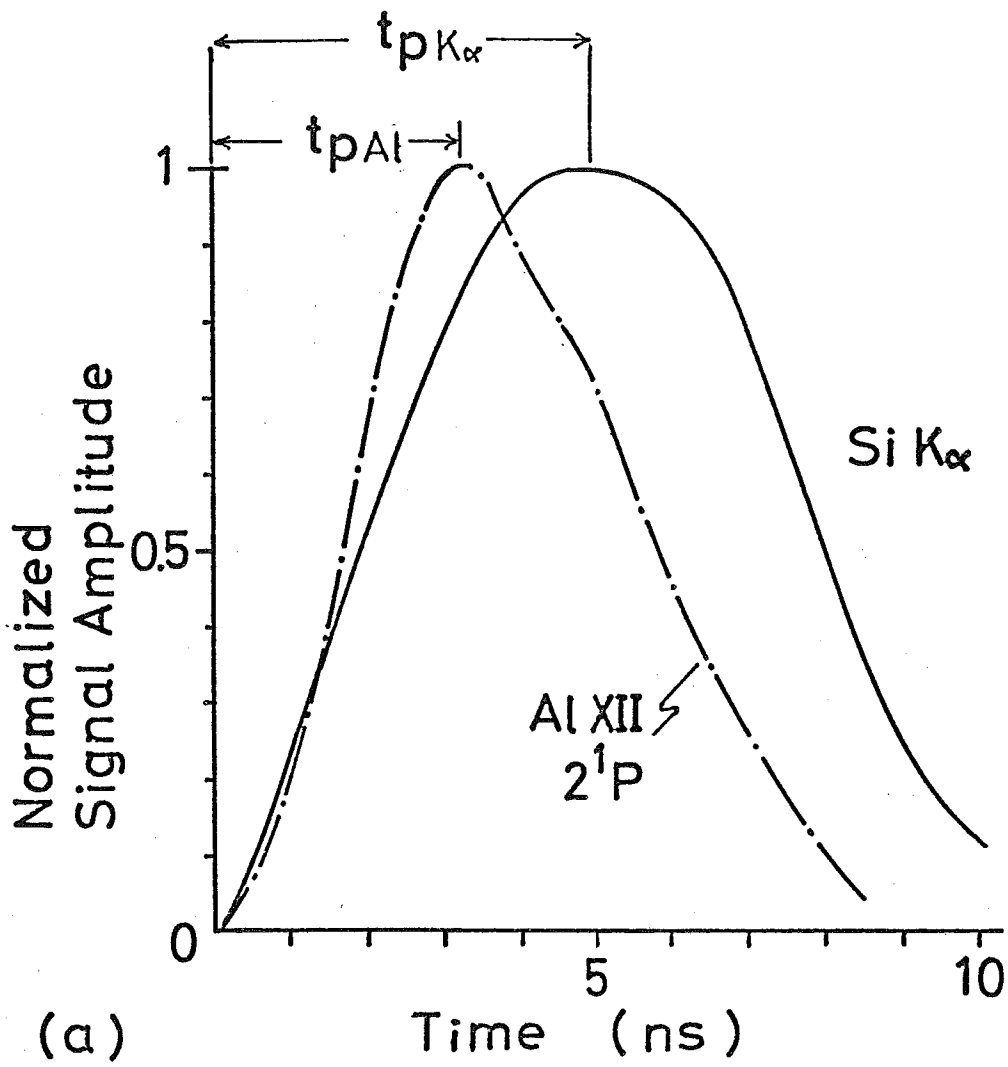
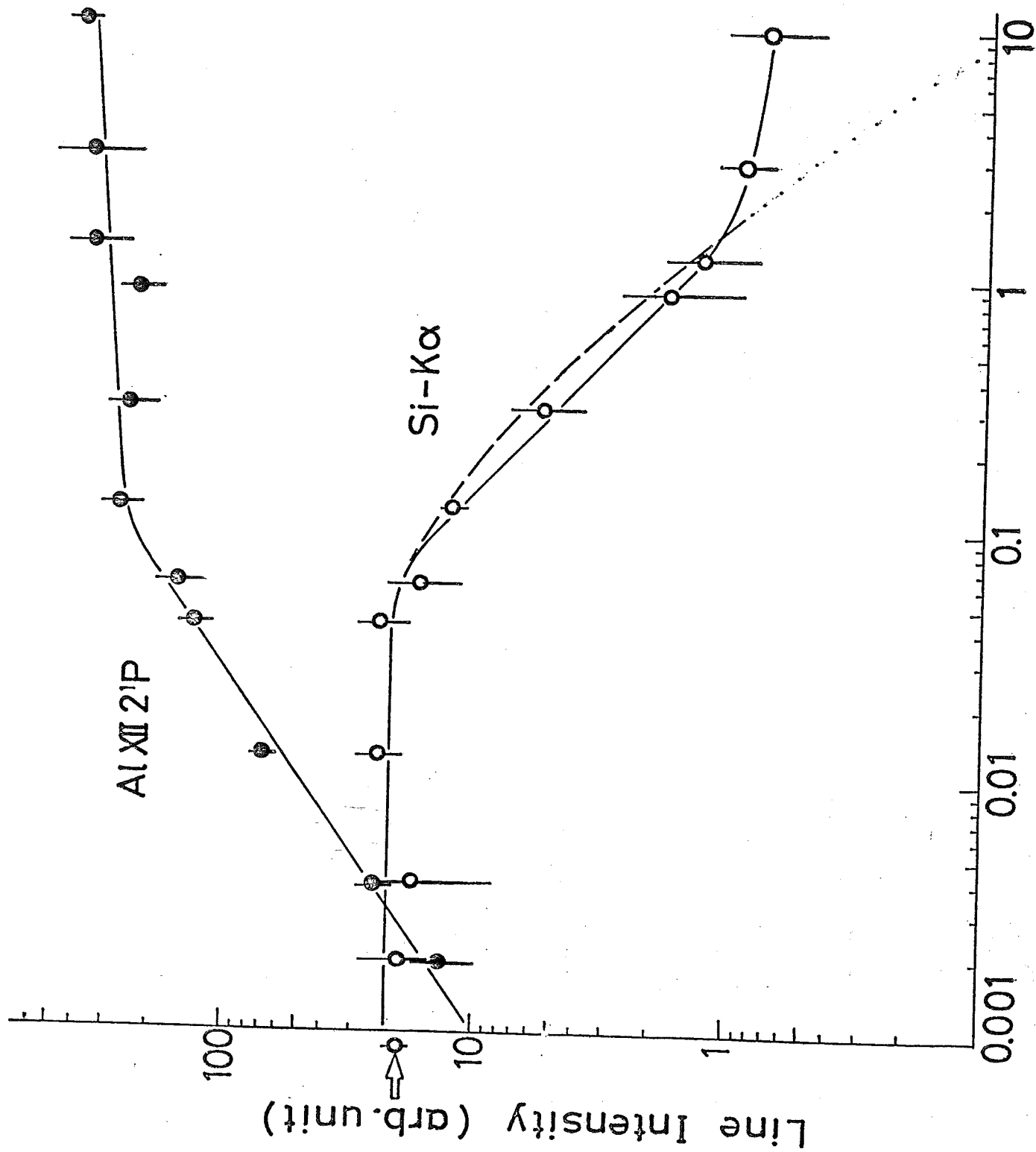


Fig.3. Naohiro YAMAGUCHI (6)



Al Layer Thickness (μm)

Fig. 4. Naohiro YAMAGUCHI ⑥

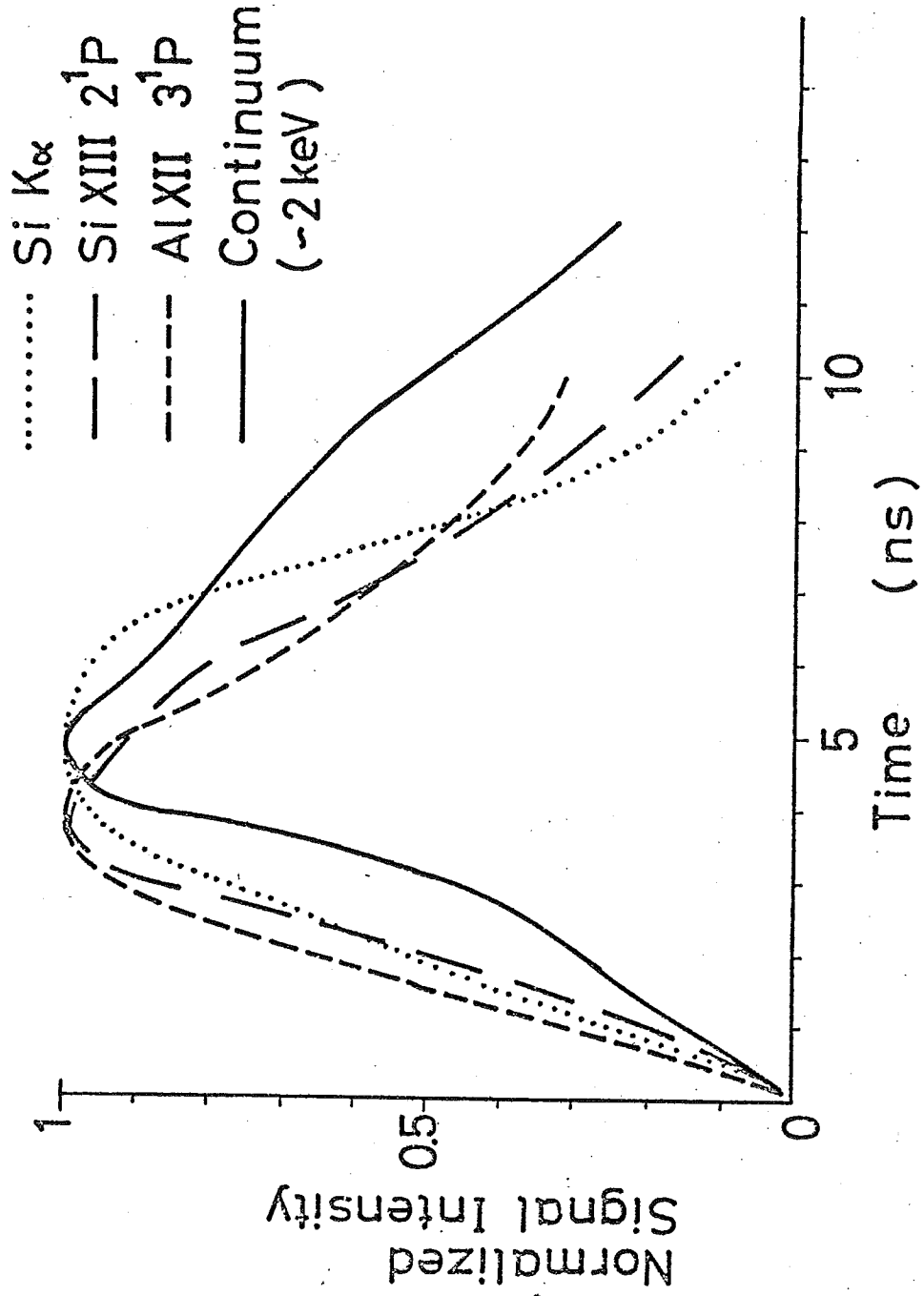


Fig.5 Naohiro YAMAGUCHI (6.5)